"Wireless Radio Frequency Detection of greatly simplified polymeric membranes based on a multifunctional Ionic Liquid"

Andrew Kavanagh[a], *Matthius Hilder*[b], *Noel Clark*[b], *Aleksandar Radu*[a] *and Dermot Diamond*[*a]

[a] *CLARITY, The Centre for Sensor Web Technologies, National Centre for Sensor Research, School of Chemical Sciences, Dublin City University, Glasnevin, Dublin 9, Ireland.*

[b] *CSIRO Materials Science and Engineering, Bayview Avenue, Clayton, Melbourne, Australia.*

Email: *Dermot.diamond@dcu.ie* Fax: +353 1 700 7995, Tel: +353 1 700 5404.

1. Abstract

In this paper, we report our ongoing investigations into the properties of *poly(vinyl)chloride (PVC)* based polymeric membranes incorporating the ionic liquid (IL) *trihexyltetradecylphosphonium dicyanamide* $[P_{6,6,6,14}][DCA]$ which fulfils several key functions - plasticiser, ligand and transducer dye. Upon co-ordination with Cu^{2+} ions, a yellow colour is generated within the membrane. Similarly exposure of a membrane to Co^{2+} ions produces a blue colour, whilst the IL is capable of co-ordinating both ions *simultaneously*, thereby generating a green optical response.

Using Wireless Radio Frequency (WRF) detection however, the inherent conducting nature of these membranes can now also be exploited as a sensor signal. WRF is a novel detection technique which monitors the conductivity of a given sample *wirelessly*, allowing non-contact detection and measurement of IL-PVC membranes as they pass through the channel. The various co-ordinated membranes produce a discriminatory drop in the resulting signal, which is a direct function of the specific metal ion (Cu^{2+}, Co^{2+} or a mixture) co-ordinated to the IL. The results of the novel WRF technique have been validated principally by electrochemical impedance spectroscopy (EIS) and also by portable x-ray fluorescence (XRF).

Keywords: Ionic Liquids, Electrochemical Sensors, Polymeric Sensors

2. Introduction

The ongoing drive for more sophisticated chemical sensing templates is based on not only the development of new materials [1, 2], but also on the engineering of new sensing instrumentation and on how the information is retrieved [3, 4]. The development of new sensing materials seems to be based on the use of single molecular probes capable of simultaneous determination of multianalytes [5, 6], and also on simultaneous detection via multiple detection channels inherent to the material studied [7-9].

At the same time, the instrument used for detection should be non-invasive on the sample, and be capable of performing multiple analyses in a short space of time. Combining these efforts represents an obvious incentive to improve many aspects of chemical sensing, such as in the remote, autonomous monitoring of analytes [10, 11].

Ionic Liquids (IL's) exhibit both a negligible vapour pressure and a wide electrochemical window [12], and have emerged as quite promising materials in both electrochemistry [13, 14] and electrochemical sensing [15]. IL's are the product of an ion-exchange metathesis reaction, resulting in a unique combination of ions that are liquid at room temperature [16, 17]. They may find use in virtually all branches of chemistry, most notably as alternative non-volatile solvents in organic synthesis [18] but also fulfilling the same role in ionic polymeric based transducers [19, 20].

Conversely IL's have been studied as co-ordinating media, with complexes of most transition and some lanthanide metals reported [21-23]. Furthermore, the ease of incorporation of IL's into a polymer support (most commonly via *in situ* polymerisation of the monomer dissolved in the IL [24] or via polymer swelling [25]) provides the basis for both solid state electrolyte [26-28] and sensing templates [29].

Our technique for the production of IL based polymer membranes involves the co-dissolution of the IL and polyvinylchloride (PVC) with Tetrahydrofuran (THF). As the solvent completely evaporates over time (12h) a transparent polymer film is produced (see experimental section).

In our previous work we described how the many favourable properties of the IL *trihexyltetradecylphosphonium dicyanamide* $[P_{6,6,6,14}][DCA]$ was incorporated into polymeric based optodes. $[P_{6,6,6,14}][DCA]$ acted as ion-exchanger, plasticizer, ligand and colorimetric dye in PVC based membranes, these membranes produced an optical response upon exposure to Cu^{2+} (yellow), Co^{2+} (blue) and both ions *simultaneously* (green) [30].

We now wish to expand on the use of IL's in polymeric membrane based sensors capable of generating optical and electrochemical signal responses. The Wireless Radio Frequency (WRF) detection instrument used in this study works particularly well for solid state, conductive samples. A signal is produced that is a direct function of the ability of the solid material to facilitate an electrical conductivity through ion movement. It has the required sensitivity, is non-invasive on the sample to be analysed and is capable of batch analyses in short spaces of time [31].

The goal of this work therefore is a proof of concept case intended to *(a)* exhibit 2-component polymeric optodes as electroactive materials capable of generating observable electrochemical signals as a result of transition metal ion binding;

and *(b)* demonstrate and validate the use of WRF detection technology by varying both components of the polymeric membrane and monitoring their inherent ionic conductivity.

The WRF instrument produces a signal in arbitrary units; its response has been validated principally by Electrochemical Impedance Spectroscopy (EIS). The level of ion coordination within the respective membrane has been characterised by X-Ray Fluorescence (XRF) Spectroscopy; which allows the reader to elucidate both observable trends in the WRF and EIS results.

3. Experimental

3.1 Chemicals and Materials

Trihexyltetradecylphosphonium dicyanamide [$P_{6,6,6,14}$][DCA] was generously donated by CYTEC® industries. Further purification was achieved by washing with both water and hexane, and by column cleansing with basic alumina [32].

Poly(vinyl)chloride (PVC), Poly(3-octylthiophene-2,5-diyl) (POT), Copper Nitrate trihydrate, Cobalt Nitrate hexahydrate, Aluminum oxide(activated, basic, Brockmann 1), Chloroform, Hexane and anhydrous Tetrahydrofuran (THF) were used as purchased from Sigma-Aldrich® Ireland Ltd.

3.2 Polymer Membrane Preparation

In order to prepare membranes; both PVC and [$P_{6,6,6,14}$][DCA] in their respective ratios (totalling 240mg) were dissolved in 3mL of anhydrous THF and left to stir for 5 minutes until completely dissolved. Once dissolved the cocktail was then poured into a glass ring bound to a glass slide by rubber bands. They were then covered and left to dry overnight.

The result is a clear, homogenous membrane of approximately 2.5cm in diameter and approximately 0.28mm in thickness. Once dry the membranes were then exposed to 1mL of a 0.1M metal ion solution for 12 hours. The metal salt solution was then removed by decanting of the liquid off the hydrophobic surface. The membrane was next dried in an oven overnight at 40^0C leaving the desired colour for analysis.

3.3 RF Wireless Conductivity Analysis

All measurements were performed using the A PCIS-3000 10-95 6536 radio frequency detector (Detection Systems, Melbourne, Australia). All measurements were performed at 83.18 kHz, the speed of the carousel was kept at 8.9 metres per minute.

The individual membranes to be analysed were initially cut to a 10 x 20mm strip. The film strip was then placed onto a non-conducting glass slide and placed inside the polystyrene container. In order to improve the accuracy of the reading, the strip was aligned vertically with the signal vector from the instrument. To further improve the accuracy of the measurement all samples were allowed to pass through the electrode channel 5 times.

The response was analysed via peak area integration; which accounts for the contribution of the whole sample to the response obtained as well as the sample dimensions. The values quoted are normalised according to the sample weight; a detailed account of how the responses were obtained can be found in figure S1.

The results of the data analysis are the values quoted below.

3.4 Electrochemical Impedance Spectroscopy

Characterization was performed using the CHI® Instruments 660A potentiostat.

Screen-printed carbon paste silver electrodes with an active electrode area of 9mm^2 were prepared in-house using a previously reported technique [33].

The electrodes were initially dropcast with a layer of POT (10^{-2}M in chloroform) in order to aid the conversion of ionic to electronic conductivity in accordance with previous works [34-36].

100μL of the membrane cocktail composition (in 1mL THF) to be analysed was then dropcast onto the silver electrode using a 1mL microsyringe. The resultant dry membranes on the electrodes were then left in their respective metal ion salt solution overnight.

The thickness of the resultant membranes were estimated using a Mitutoyo® micrometer calibrated to a resolution of 1μm.

The impedance measurements were performed in the frequency range of 1 MHz to 0.01 Hz with a perturbation signal of 100mV. The reference electrode used was an aqueous Ag/AgCl (CHI® Instruments 111, surface area: 3.14 mm^2).
A platinum wire electrode (CHI® Instruments 115, surface area: 3.14 mm^2) was used as the counter. A 1nF capacitance shunt was used to reduce high frequency noise.

In order to obtain the impedance of the non-complexed membrane, the electrode in question was placed in 6ml of a 0.1M KCl solution. K^+ is a soft, non-coordinating cation, and with no reported complexation behaviour with $[DCA]^-$.

3.5 Portable XRF Measurements

Measurements were performed using the Thermo NITON® portable XRF analyser, using the standard thin film mode. In order to improve the accuracy of the measurement a batch reading of 3 x 180secs was performed. The averages of these measurements are the values quoted below.

4. Results and Discussion

4.1 Membrane Components

Dicyanamide (DCA)$^-$ has previously been termed a pseudohalide with rather complex binding stoichiometry [37]. Complexation of this ligand with heavy metals results in net neutral complexes of 1, 2 and 3 dimensions [38, 39] plus electrochemically neutral co-ordinated polymers [40]. It was first used as an anion for IL's as its extensive electron delocalisation meant it only exhibited electrostatic interactions with the IL cation; resulting in a liquid with a comparably low viscosity[41].

Solid, hydrophobic, polymeric membranes of this nature are typical of those used in Ion-Selective Electrodes (ISE's) [42], a type of electrochemical sensor used for the determination of trace amounts of ions in solution. As the analysis typically involves the migration of an analyte between an aqueous phase and the hydrophobic polymeric surface, the mechanism of ion-transfer must be taken into account.

In our previous work we have detailed that the migration mechanism of metal ions from aqueous to organic phase is co-extraction of the metal and its counter ion into the membrane rather than the ion-exchange convention [30]. In this case as the metal ion transfers through the polymeric membrane boundary it complexes and neutralises the anionic ligand; the counter ion of the metal salt (NO_3) must therefore cross the membrane boundary in order to preserve electroneutrality within the membrane.

The two principal components used in ISE membranes are the polymer and the plasticiser. Depending on the analytical approach, the w/w ratio of these can vary greatly, although a ratio of 2:1 plasticiser: polymer (w/w) is generally accepted as the optimum. Changing the IL-polymer ratio can significantly influence important characteristics such as physical stability and elasticity [43]. In order to elucidate what affect the ratio of components will impart on the resulting conductivity and binding levels, the amounts of $[P_{6,6,6,14}][DCA]$ were varied from 66wt% to 50wt% and 33wt%. The characteristics of the resulting membranes were then investigated using WRF, EIS and XRF.

4.2 Membrane Component Ratio 2:1, IL:PVC.

The WRF detector system used in this study utilises radio frequency technology in order to obtain the conductivity of a sample as it passes through a defined point.

This point is the transmitting electrode, which passes a low voltage, low-frequency AC signal toward a receiving electrode *wirelessly*. The sample to be analysed is housed in an insulating polystyrene based container which is placed on a miniature conveyor (Fig 1).

The insulating container with the sample placed inside is then allowed to pass through the electrode channel where it is processed and analysed via a PC. It has been used to great effect previously for the wireless detection of acetic acid and ammonia vapour using ink-jet printed polyaniline dispersions [31].

Figure 2 shows results obtained for a set of membranes containing a component ratio of 2:1, IL: PVC. Firstly a "blank" membrane (i.e. no metal ion exposure) was allowed to pass through the electrode channel. Next, three membranes individually exposed to (a) Cu^{2+}, (b) Co^{2+} and finally (c) a solution containing a mixture of both ions were then allowed to pass through the electrode channel.

One can see from Figure 2 the response obtained for the blank membrane (bold, dashed line). It demonstrates that this membrane is indeed electroactive (due to the

presence of the IL) as the WRF instrument proved capable of detecting it as it passed through the electrode channel.

What is also interesting to observe is the signal reduction seen for the respective co-ordinated membranes, which ultimately means that they have become less conductive. This downward trend is most likely due to the co-ordinating chemistry of $[DCA]^-$; as previously discussed. The observed signal trend is Cobalt > Mix > Copper which we believe is directly related to the level of ion transfer and co-ordination within the membrane; which will be discussed later in this text.

Some features inherent to this technique are so called "edge effects" which occur as the sample container first enters and leaves the electrode channel. These signals occur as the dielectric constant of the insulating housing material changes upon initial and final contact with the voltage vector. This, coupled with the signal produced from the conductive strip, means that the graph obtained is an effective picture of the dimensions of the container as it passes through the channel, with the conductive sample housed safely inside. A summary of the peak area integration analysis can be seen below (table 1) and in figure S2.

WRF detection is a novel technique producing peak heights of arbitrary units, and therefore its results must be validated appropriately. For this purpose, Electrochemical Impedance Spectroscopy (EIS) was employed, as this provides an independent estimation of the sample conductivity in S/cm.

The resulting x-axis intercept of the *Nyquist* plot (fig 3.) is used to determine the resistance of charge transfer (R_{CT}) of the membrane, which is then easily converted to the corresponding conductivity via the equations:

$$G = 1/R \quad \textbf{(1)}$$

$$\sigma = GL/A \quad \textbf{(2)}$$

where G is the conductance, R is the resistance, σ is the conductivity, A is the cross sectional area of the working electrode and L is the estimated thickness of the polymer membrane on the electrode [44, 45].

Our screen printed, in-house electrodes have a cross sectional area of $9mm^2$ [33]. In order to estimate the average thickness of the membrane; a Mitutoyo® micrometer calibrated to a resolution of 1μm was used. The results of the thickness analysis across 6 electrodes can be seen in figures S3-S5. Table 2 provides a summary of the results obtained.

One can see from both figure 3 and table 2 that the impedance of the metal ion co-ordinated membranes has increased. Here the trend is inverted from the previous result obtained. In order to see how the response from the two instruments correlate, plots of both % decrease (WRF) and % increase (EIS) of the signal response vs. the samples were constructed (Figure S6). Both trends are effectively linear and complement each other. EIS is therefore an effective validation of the novel WRF

instrumental result; whilst also providing an independent estimation the increase in response seen.

We believe that the inverse trends seen must be related to the level of co-ordination within the membrane. In order to confirm this; XRF was then finally used. We have also seen previously in our optical characterisation that whilst [$P_{6,\ 6,\ 6,\ 14}$] [DCA] is capable of binding to both Co^{2+} and Cu^{2+}, its preferentiality is toward Cu^{2+}. Again for this analysis, membranes containing the same component ratio were analysed and the metal salt solutions concentration were also kept constant.

Figure 4 (above) depicts the spectra obtained; the first feature to note is that the peak height obtained for chlorine is approximately the same for all 4 membranes. This illustrates that the ratio of PVC is indeed kept constant for all measurements, and so acts as an internal standard. The peaks for both Cobalt and Copper are also labelled, it can be seen that the peak height is considerably higher for Copper over Cobalt, which is indicative of the binding preferentiality of the IL.

The peak heights obtained for the mixture are also labelled; they are, of course lower than those obtained for the pure ion solutions. The reduction in peak height is more dramatic for Cobalt over Copper, and given that the initial metal salt solution contained a volume ratio of 2:1, Co^{2+}:Cu^{2+}, further strengthens our binding preferentiality argument.

Not unlike its instrumental equivalent, the portable XRF analyser is also capable of quantifying the intensity of the fluorescent peak levels into parts per million concentrations (ppm) [46, 47]. The calculation is based on many factors, but is most heavily dependent on the weight fraction of the element in the membrane and the dimensions of the sample [48]. The quantitative results of the first set of XRF analyses are detailed in table 2. From this table it is easy to deduce that even though all of the membranes were exposed to the same concentration of metal ion solution, that the uptake of Copper is significantly higher than Cobalt (~2.2 times greater).

4.3 Membrane Component Ratio 1:1, IL:PVC.

Increasing the amount of polymer in the membrane to 50wt% led to membranes with slightly reduced flexibility and elasticity. The polymer can also be viewed as an insulating matrix, so the resulting measured impedance should also increase; whilst the wireless conductivity signals should also decrease. Equally, by reducing the amount of IL, the availability of binding sites is lessened; so the competition for one binding site between two analytes increases.

Table 5 (top) lists the values obtained from the WRF analysis. Once again; they are the result of peak area integration and mass correction analysis of the response obtained (figure S10 (a)).

In the first instance; the conductivity values are uniformly shifted down. This is to be expected; as the concentration ratio of the IL has been reduced. The selective downward trend based on the nature of metal ion co-ordination still remains.

Both WRF and EIS still complement each other in that the inverse trend of increased impedance for the co-ordinated membranes is still evident. This can be seen by looking at figure 5 (left) and table 4 (top) which summarises the results. What can also be observed is that the impedance for all membranes is significantly increased due to the increased concentration of PVC. Once again a correlation analysis of the respective responses from both EIS and WRF was undertaken (Figure S7). Again both trends are linear and serve to complement both techniques.

A summary of the XRF analysis can be seen in table 6 (top). XRF once again proves to be a valid tool to explain the EIS and WRF results obtained previously. The levels of both Cu and Co in the membrane serve to validate both the conductivity and impedance trends seen for both WRF and EIS respectively. Once again Cu levels prevail over Co in all cases, which again are a reflection of the co-ordinating chemistry of the ligand $[DCA]^-$.

What is interesting to note from both EIS and XRF analyses; is that the selectivity of the IL for Cu^{2+} over Co^{2+} has increased substantially when compared to the first case studied. This is most likely a combination of the decreased concentration of binding sites resulting in an increased competition between two analytes for one ligand plus also the fact that we have consistently observed a higher preference of the membranes for Cu^{2+} over Co^{2+}.

4.4 Membrane Component Ratio 1:2, IL:PVC.

By further increasing the concentration of PVC to 66wt%, the resulting membranes became more inflexibile and brittle. A further reduced IL content means they have become primarily hydrophobic, which will impede their ability to uptake and bind metal ions.

This proved to be a hindrance for the WRF detection system; a summary of the results obtained can be viewed in table 5 (bottom) and figure S10 (b). Given that its response is based on the conductivity of a given sample, it proved capable of only detecting the "blank" membrane containing only 33w% IL. Any co-ordination that does occur within this particular set of membranes results in neutral co-ordinated networks; which will lower the conductivity even further. This had the result of lowering the conductivity outside the limitation of the WRF instrumental setup. This is a limitation of the current setup and will be the subject of future work.

Again; the EIS spectra yielded no observable trend (Figure 5 (right) and table 4 (bottom)). The impedance for all membranes is again increased (approx. one order of magnitude) due to increasing the levels of PVC within the membrane.

From the individual *Bode* plots -*which depict the relationship between the modulus of impedance and the scanning frequency*- the impedance shift for the blank membrane is linear for both IL and PVC concentrations, which can be seen in figures S8 and S9.

The XRF analysis proved helpful to validate the previously unexpected EIS trend (Table 6 (bottom)). Here the highest concentration of metal in the membrane was found to be the mixture, which corresponds to the highest impedance response seen for these membranes. The next highest levels are seen for Cu, whilst Co levels proved undetectable which correlates perfectly with the EIS response trend. The EIS spectra obtained are therefore directly related to the level of ion transfer and co-ordination within the membrane.

5. Conclusion

In this work we have demonstrated that our IL based membranes do act as electroactive materials which; when co-ordinated to heavy metals provide a measured sensor response. We have also effectively demonstrated the use of WRF technology for this purpose and shown how the results obtained from 3 differing techniques definitively summarise the inherent co-ordinating chemistry of these membranes.

In this case the IL based polymeric optodes are capable of discriminatory co-ordination of the heavy metals Cu^{2+}, Co^{2+} and both ions in a mixture which produces an equal discriminatory conductivity decrease in the WRF signal. By documenting the inverse trend of impedance, we have validated this novel conductivity result. Both the WRF and EIS trends were then easily explained by studying the level of ion transfer and the co-ordinating preferences of the IL ligand $[DCA]^-$. This was achieved by quantifying the amount of metal present in the membrane using XRF.

By examining the case of Cu^{2+} co-ordination; the three detection techniques can be summarised as follows: Cu^{2+} exhibits the highest binding preferentiality to the IL (XRF), thereby producing the lowest WRF signal and the highest EIS response. The opposite then applies for Co^{2+} co-ordination with the mixture inevitably in between.

With this and our previous work, we have now effectively shown how incorporation of a ligand as part of an IL can dramatically simplify a polymeric based optode's composition, and how both the inherent optical and transduction processes can be monitored using a variety of detection techniques.

As we have now gained a valid insight into the electrical effects of metal- ion co-ordination in polymeric membranes through variation of its constituents; future work

will be aimed at optimising important analytical characteristics such as the effects of changing of the IL cation and optimising the effects of analyte concentration.

As mentioned previously IL's have been shown to bind to a range of d-block elements, plus important target analytes such as CO_2 [49], benzaldehyde and acetone [50]. Recently they have been shown to act as direct sensing materials for acids in aqueous and non-aqueous environments[51].

If a change in conductivity can be presumed upon binding to the analyte, then the inherent conductivity properties of IL's should also change. The use of wireless conductivity monitoring also has many potential advantages, such as remote, autonomous monitoring. By combining the many advantageous properties of both IL's and conductivity detection, then dramatic gains in sensing materials AND detection can be achieved.

6. Acknowledgements

This work is supported by Science Foundation Ireland under grant 07/CE/I1147 including the SFI-funded National Access Programme (NAP) grant NAP210 and by Enterprise Ireland grant 07/RFP/MASF812, which is part of EU-MATERA initiative.

AK and AR would like to thank Dr. Al Robertson from CYTEC® Industries for the generous donation of the IL used in this work. AK and AR would also like to thank Prof. Robert Forster and Dr.Colm Fallon of DCU for their kind use of instruments and guidance for the duration of this work, as well as DCU for the Research Career Start Programme award.

7. Appendices

Electronic Supplementary Information (ESI) available. WRF peak integral and mass correction analyses. Membrane thickness analyses on the working electrode plus EIS spectra on the effect of component ratio.

8. References

1. A. Aghaei, M. R. M. Hosseini and M. Najafi,Electrochim. Acta, 55 1503-1508.
2. N. Zine, J. Bausells, F. Vocanson, R. Lamartine, Z. Asfari, F. Teixidor, E. Crespo, I. A. M. de Oliveira, J. Samitier and A. Errachid,Electrochim. Acta, 51 (2006) 5075-5079.
3. L. Yang, R. W. Zhang, D. Staiculescu, C. P. Wong and M. M. Tentzeris,Ieee Antennas and Wireless Propagation Letters, 8 (2009) 653-656.
4. Y. Kim, R. G. Evans and W. M. Iversen,Ieee Transactions on Instrumentation and Measurement, 57 (2008) 1379-1387.
5. N. Kaur and S. Kumar,Chemical Communications, (2007) 3069-3070.
6. N. Kaur and S. Kumar,Tetrahedron Letters, 49 (2008) 5067-5069.
7. D. Jimenez, R. Martinez-Manez, F. Sancenon, J. V. Ros-Lis, J. Soto, A. Benito and E. Garcia-Breijo,European Journal of Inorganic Chemistry, (2005) 2393-2403.
8. D. Jimenez, R. Martinez-Manez, F. Sancenon and J. Soto,Tetrahedron Letters, 45 (2004) 1257-1259.
9. S. E. Andria, C. J. Seliskar and W. R. Heineman,Analytical Chemistry, 82 1720-1726.
10. J. Cleary, C. Slater, C. McGraw and D. Diamond,Ieee Sensors Journal, 8 (2008) 508-515.
11. C. M. McGraw, S. E. Stitzel, J. Cleary, C. Slater and D. Diamond,Talanta, 71 (2007) 1180-1185.
12. M. Galinski, A. Lewandowski and I. Stepniak,Electrochim. Acta, 51 (2006) 5567-5580.
13. C. Zhao, G. Burrell, A. A. J. Torriero, F. Separovic, N. F. Dunlop, D. R. MacFarlane and A. M. Bond,Journal of Physical Chemistry B, 112 (2008) 6923-6936.
14. M. Armand, F. Endres, D. R. MacFarlane, H. Ohno and B. Scrosati,Nature Materials, 8 (2009) 621-629.
15. M. H. Yang, B. G. Choi, H. Park, W. H. Hong, S. Y. Lee and T. J. Park,Electroanalysis, 22 1223-1228.
16. K. J. Fraser and D. R. MacFarlane,Australian Journal of Chemistry, 62 (2009) 309-321.
17. C. Chiappe and D. Pieraccini,Journal of Physical Organic Chemistry, 18 (2005) 275-297.
18. S. Chowdhury, R. S. Mohan and J. L. Scott,Tetrahedron, 63 (2007) 2363-2389.
19. M. D. Bennett and D. J. Leo,Sensors and Actuators a-Physical, 115 (2004) 79-90.
20. M. D. Bennett, D. J. Leo, G. L. Wilkes, F. L. Beyer and T. W. Pechar,Polymer, 47 (2006) 6782-6796.
21. H. Mehdi, K. Binnemans, K. Van Hecke, L. Van Meervelt and P. Nockemann,Chemical Communications, 46 234-236.

22. P. Nockemann, M. Pellens, K. Van Hecke, L. Van Meervelt, J. Wouters, B. Thijs, E. Vanecht, T. N. Parac-Vogt, H. Mehdi, S. Schaltin, J. Fransaer, S. Zahn, B. Kirchner and K. Binnemans,Chemistry-a European Journal, 16 1849-1858.
23. K. Lunstroot, K. Driesen, P. Nockemann, K. Van Hecke, L. Van Meervelt, C. Gorller-Walrand, K. Binnemans, S. Bellayer, L. Viau, J. Le Bideau and A. Vioux,Dalton Transactions, (2009) 298-306.
24. T. Ueki and M. Watanabe,Macromolecules, 41 (2008) 3739-3749.
25. P. Izak, S. Hovorka, T. Bartovsky, L. Bartovska and J. G. Crespo,Journal of Membrane Science, 296 (2007) 131-138.
26. F. Gayet, L. Viau, F. Leroux, S. Monge, J. J. Robin and A. Vioux,Journal of Materials Chemistry, 20 9456-9462.
27. V. Armel, D. Velayutham, J. Z. Sun, P. C. Howlett, M. Forsyth, D. R. MacFarlane and J. M. Pringle,Journal of Materials Chemistry, 21 (2011) 7640-7650.
28. T. E. Sutto, T. T. Duncan, T. C. Wong and K. McGrady,Electrochim. Acta, 56 (2011) 3375-3379.
29. S. Y. Yang, F. Cicoira, R. Byrne, F. Benito-Lopez, D. Diamond, R. M. Owens and G. G. Malliaras,Chemical Communications, 46 7972-7974.
30. A. Kavanagh, R. Byrne, D. Diamond and A. Radu,Analyst, 136 (2010) 348-353.
31. N. B. Clark and L. J. Maher,Reactive & Functional Polymers, 69 (2009) 594-600.
32. T. Ramnial, S. A. Taylor, M. L. Bender, B. Gorodetsky, P. T. K. Lee, D. A. Dickie, B. M. McCollum, C. C. Pye, C. J. Walsby and J. A. C. Clyburne,Journal of Organic Chemistry, 73 (2008) 801-812.
33. A. Morrin, A. J. Killard and M. R. Smyth,Analytical Letters, 36 (2003) 2021-2039.
34. A. Kavanagh, R. Copperwhite, M. Oubaha, J. Owens, C. McDonagh, D. Diamond and R. Byrne,Journal of Materials Chemistry, 21 (2011) 8687-8693.
35. J. Bobacka, A. Ivaska and A. Lewenstam,Electroanalysis, 15 (2003) 366-374.
36. S. A. D. Cicmil, A. Kavanagh, D. Diamond,U. Mattinen, J. Bobacka, and A. L. a. A. Radu,Electroanalysis,(2011), DOI: 10.1002/elan.201100137.
37. S. R. Batten and K. S. Murray,Coordination Chemistry Reviews, 246 (2003) 103-130.
38. W. Dong, M. Liang, Y. Q. Sun and Z. Q. Liu,Z. Anorg. Allg. Chem., 629 (2003) 2443-2445.
39. L. F. Jones, L. O'Dea, D. A. Offermann, P. Jensen, B. Moubaraki and K. S. Murray,Polyhedron, 25 (2006) 360-372.
40. J. L. Manson, A. M. Arif, C. D. Incarvito, L. M. Liable-Sands, A. L. Rheingold and J. S. Miller,Journal of Solid State Chemistry, 145 (1999) 369-378.
41. D. R. MacFarlane, J. Golding, S. Forsyth, M. Forsyth and G. B. Deacon,Chemical Communications, (2001) 1430-1431.
42. E. Bakker, P. Buehlmann and E. Pretsch,Chemical Reviews, 97 (1997) 3083-3132.
43. N. V. Shvedene, D. V. Chernyshov, M. G. Khrenova, A. A. Formanovsky, V. E. Baulin and I. V. Pletnev,Electroanalysis, 18 (2006) 1416-1421.

44. P. E. Stallworth, J. J. Fontanella, M. C. Wintersgill, C. D. Scheidler, J. J. Immel, S. G. Greenbaum and A. S. Gozdz,Journal of Power Sources, 81 (1999) 739-747.
45. L. A. Neves, J. Benavente, I. M. Coelhoso and J. G. Crespo,Journal of Membrane Science, 347 42-52.
46. S. H. Hosseini and A. A. Entezami,Journal of Applied Polymer Science, 90 (2003) 49-62.
47. M. Vazquez, K. Mikhelson, S. Piepponen, J. Rama, M. Sillanpaa, A. Ivaska, A. Lewenstam and J. Bobacka,Electroanalysis, 13 (2001) 1119-1124.
48. B. Beckhoff, *Handbook of Practical X-Ray Fluorescence Analysis*, Springer, 2006.
49. E. D. Bates, R. D. Mayton, I. Ntai and J. H. Davis,Journal of the American Chemical Society, 124 (2002) 926-927.
50. M. C. Tseng and Y. H. Chu,Chemical Communications, 46 2983-2985.
51. Q. Zhang, S. Zhang, S. Liu, X. Ma, L. Lu and Y. Deng,Analyst, 136 (2011) 1302-1304.

Supplementary Information

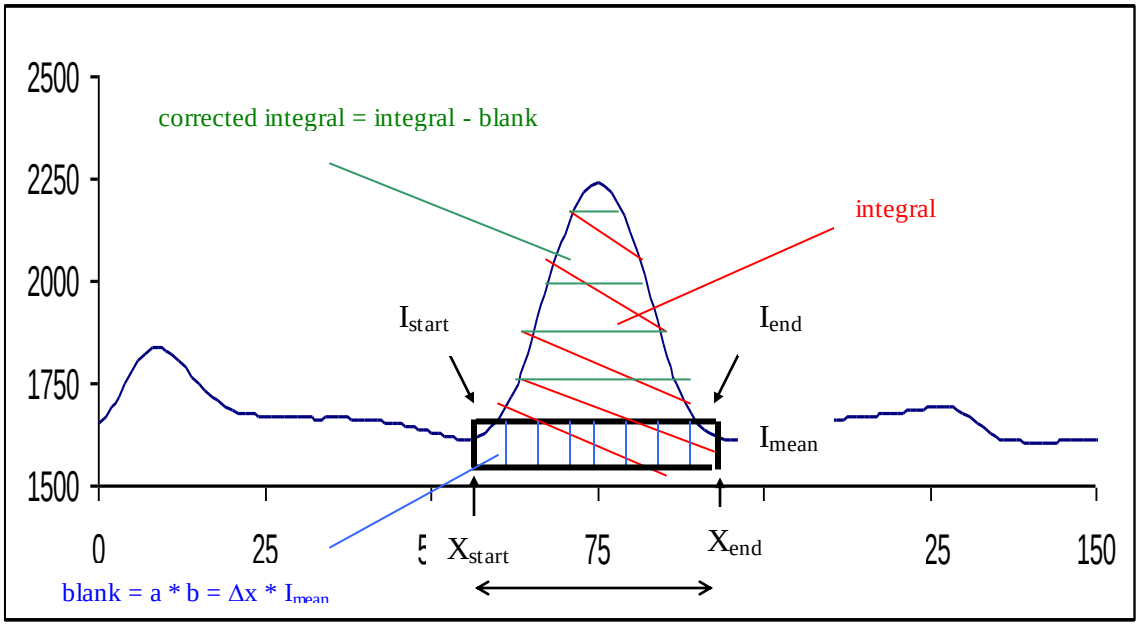

Figure S1: Details of peak area analysis used in WRF analysis

- First the intensity value is taken at the beginning (I_{start}) of the signal peak, at the end (I_{end}), and a mean (I_{mean}) of the two.
- The x-axis parameter values are also taken i.e. X_{start} and X_{end}, and the difference between them ΔX.
- In order to obtain a background or blank value, the area with dimensions of I_{mean} x ΔX is calculated.
- The integral is obtained by adding together each intensity value from I_{start} to I_{end} (Integral Raw).
- The intergral is then corrected by each individual mass reading, and by subtracting the background value.

	Mass: (g)	I_{start}	I_{end}	I_{mean}	X_{start}	X_{end}	ΔX	***Blank***	***Integral (raw)***	***Integral (mass corrected)***
Blank	0.2309	1638.9	1611.6	1625.25	56	95	39	63384.75	75503.8	52486.14
Copper	0.2221	1636.2	1632	1634.1	52	91	39	63729.9	72456.8	39292.66
Cobalt	0.2317	1625.6	1629.4	1627.5	48	89	41	66727.5	76801.8	43479.93
Mix	0.2277	1629.2	1633	1631.1	47	89	42	68506.2	77675.17	40267.75

Figure S2: WRF Peak area analysis for membranes containing IL:PVC, 2:1.

	electrode thickness		*electrode + membrane thickness*	*membrane thickness*
	mm		mm	mm
1	0.24	1	0.34425	0.11175
2	0.23	2	0.34825	0.11575
3	0.23	3	0.33225	0.09975
4	0.23	4	0.32925	0.09675
5	0.24	5	0.33525	0.10275
6	0.225	6	0.34425	0.11175
average	0.2325	7	0.34925	0.11675
stdev	0.006123724	8	0.36725	0.13475
		9	0.34375	0.11125
			average membrane thickness	0.111
			stdev	0.011

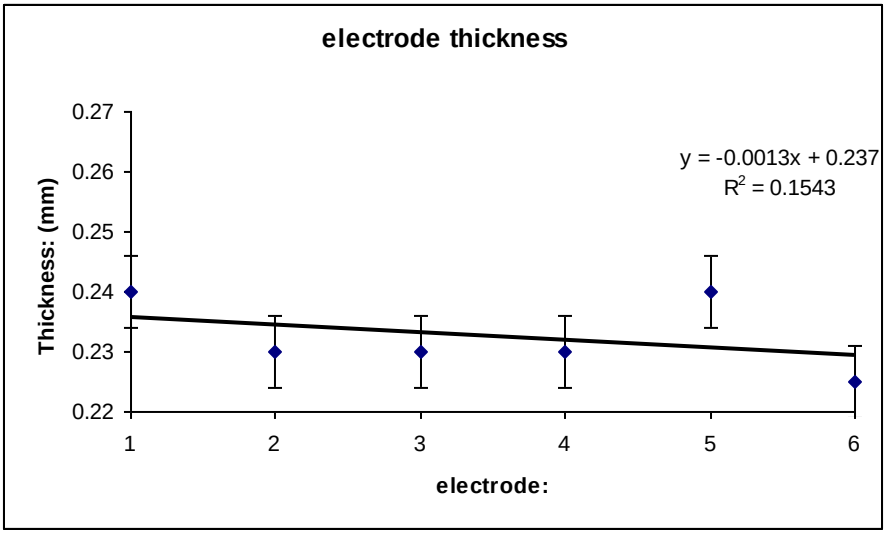

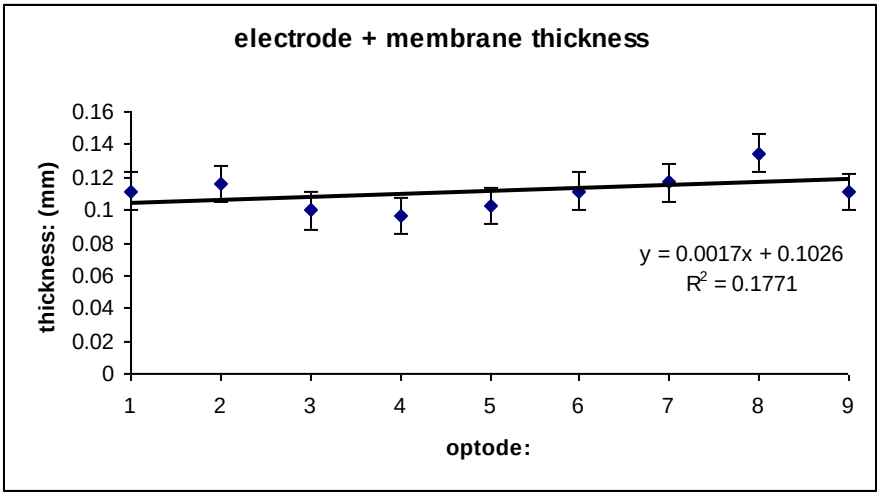

Figure S3: Electrode and membrane thickness analysis for membranes containing 33wt% PVC.

	electrode thickness
	mm
1	0.24
2	0.23
3	0.23
4	0.23
5	0.24
6	0.225
average	0.2325
stdev	0.006123724

	electrode + membrane thickness
	mm
1	0.5965
2	0.6215
3	0.5425
4	0.5615
5	0.5355
6	0.5435
7	0.5705
8	0.5405
9	0.5395
average	0.561
stdev	0.0299
average membrane thickness	***0.328***

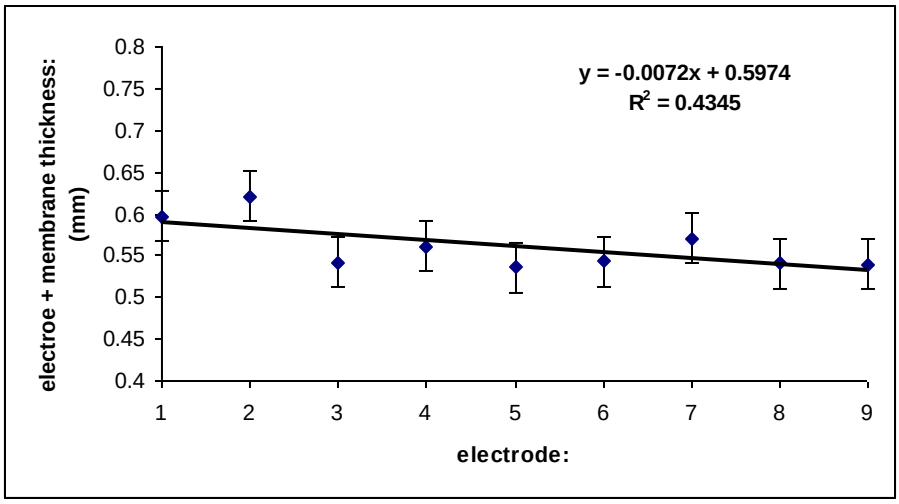

Figure S4: Electrode and membrane thickness analysis for membranes containing 50wt% PVC.

	electrode thickness
	mm
1	0.24
2	0.23
3	0.23
4	0.23
5	0.24
6	0.225
average	0.2325
stdev	0.006123724

	electrode + membrane thickness
	mm
1	0.66625
2	0.64825
3	0.66925
4	0.62525
5	0.59625
6	0.65825
7	0.63925
8	0.64525
9	0.65325
average	0.644
stdev	0.022
average membrane thickness	***0.412***

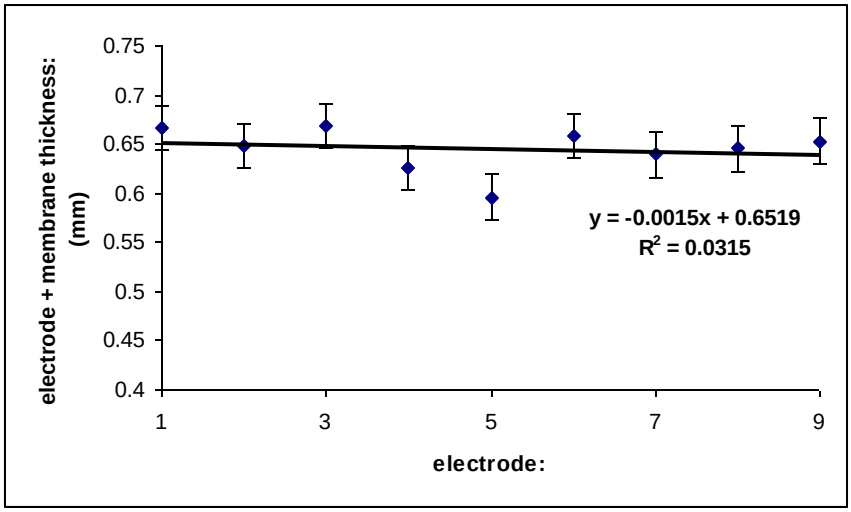

Figure S5: Electrode and membrane thickness analysis for membranes containing 66wt% PVC.

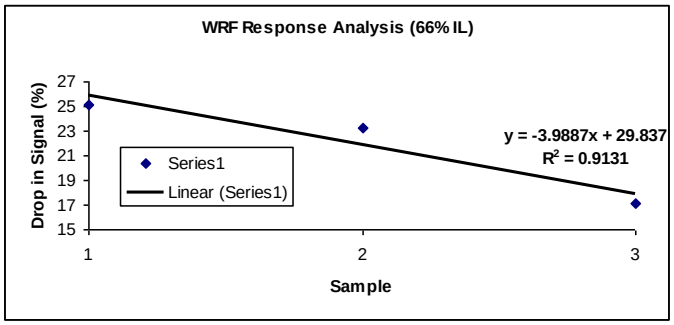

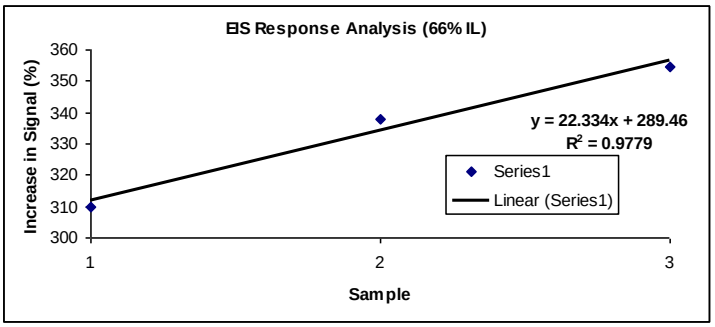

2:1 IL:PVC

	WRF			% Drop
Blank	52486			
Copper	39292	13194	1	25.13813
Mix	40267	12219	2	23.28049
Cobalt	43479	9007	3	17.16077

	EIS			% increase
Blank	3694			
cobalt	15140	11446	1	309.853817
Mix	16180	12486	2	338.0075799
Copper	16790	13096	3	354.5208446

Figure S6: Detailed analysis of response obtained for membranes containing 2:1 (IL : PVC). Here the parameters on the x-axes represent (for WRF) 1 = Copper; 2 = Mix and 3 = Cobalt. For EIS; 1 = Cobalt, 2= Mix and 3 = Copper.

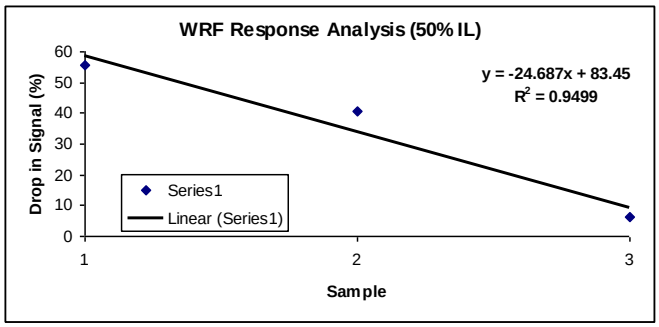

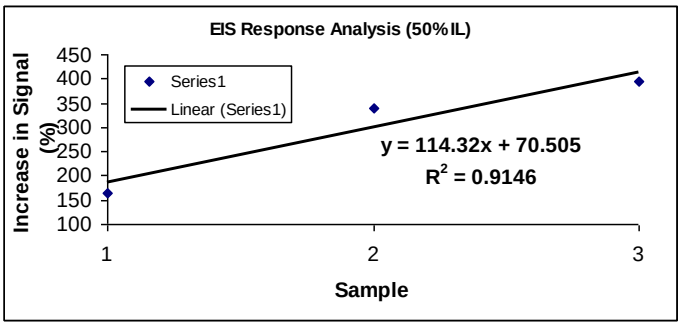

1:1 IL:PVC

	WRF			
Blank	15879			
Copper	7068	8811	1	55.48838
Mix	9428	6451	2	40.62598
Cobalt	14908	971	3	6.114995

	EIS			
Blank	47760			
cobalt	126400	78640	1	164.6566
Mix	209900	162140	2	339.4891
Copper	235600	187840	3	393.2998

Figure S7: Detailed analysis of response obtained for membranes containing 2:1 (IL : PVC). Here the parameters on the x-axes represent (for WRF) 1 = Copper; 2 = Mix and 3 = Cobalt. For EIS; 1 = Cobalt, 2= Mix and 3 = Copper.

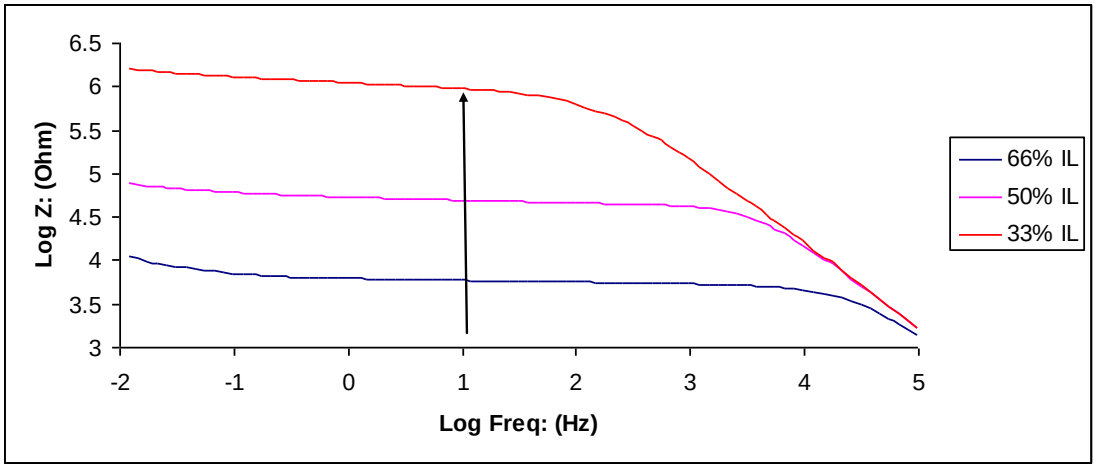

Figure S8: Bode plot's obtained for increasing IL concentrations

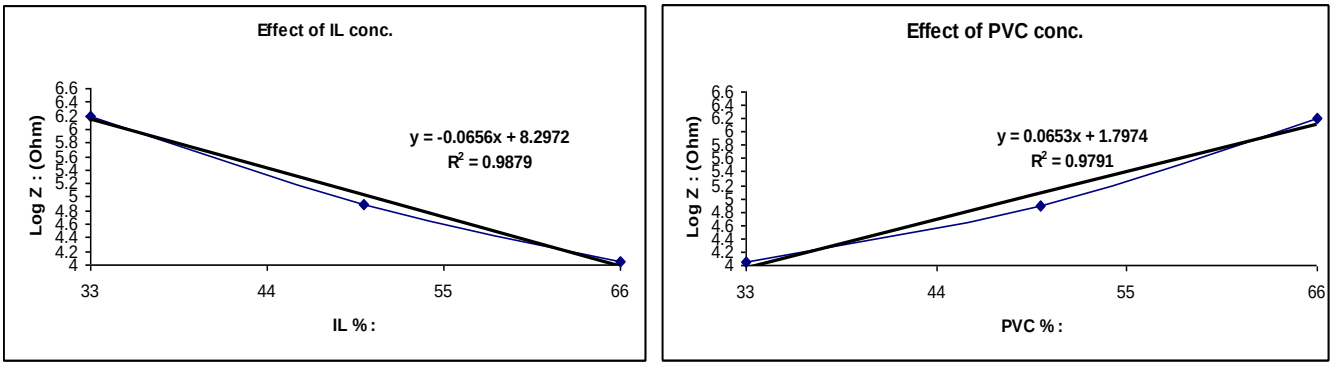

Figure S9: Top: Plot of Impedance versus IL concentration (left) and PVC concentration (right).

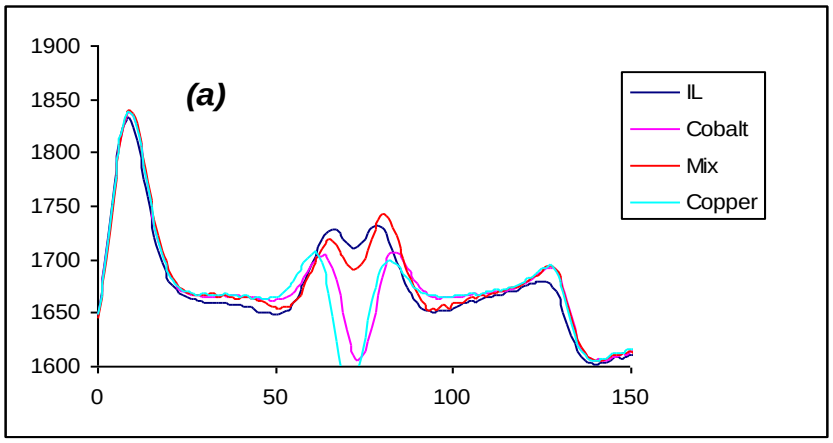

	Mass: (g)	***I_{start}***	***I_{end}***	***I_{mean}***	***X_{start}***	***X_{end}***	***ΔX***	***Blank***	***Integral (raw)***	***Integral (mass corrected)***
Blank	0.2284	1650	1650	1650	52	94	42	69300	72931	15879
Copper	0.2248	1665	1665	1665	43	87	44	73260	74849	7068
Cobalt	0.226	1656	1654	1655	54	96	42	69510	72879	14908
Mixture	0.2106	1663	1665	1666.5	45	87	42	71552	73537	9428

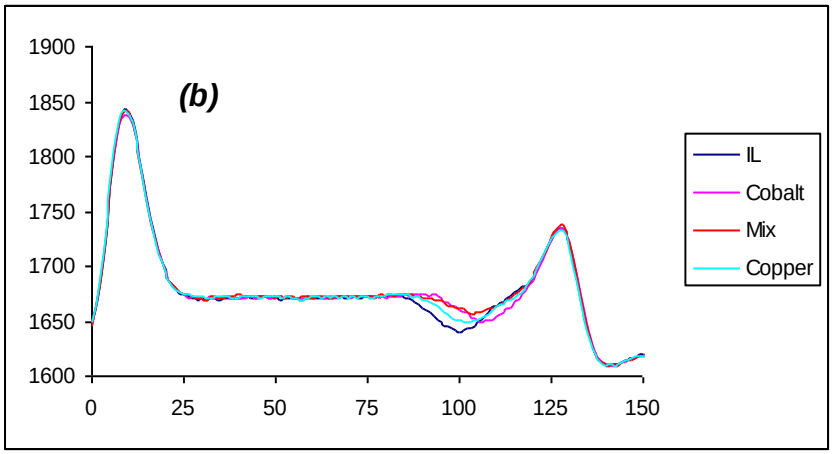

	Mass: (g)	I_{start}	I_{end}	I_{mean}	X_{start}	X_{end}	ΔX	***Blank***	***Integral (raw)***	***Integral (mass corrected)***
Blank	0.226	1669.4	1670.5	1670	34	56	22	40171.2	38435	7502
Copper	0.2325	-	-	-	-	-	-		-	-
Mix	0.233	-	-	-	-	-	-		-	-
Cobalt	0.2243	-	-	-	-	-	-		-	-

Figure S10: WRF response obtained for (a) membranes containing 1:1, IL: PVC and (b) 1:2, IL: PVC.

Figures:

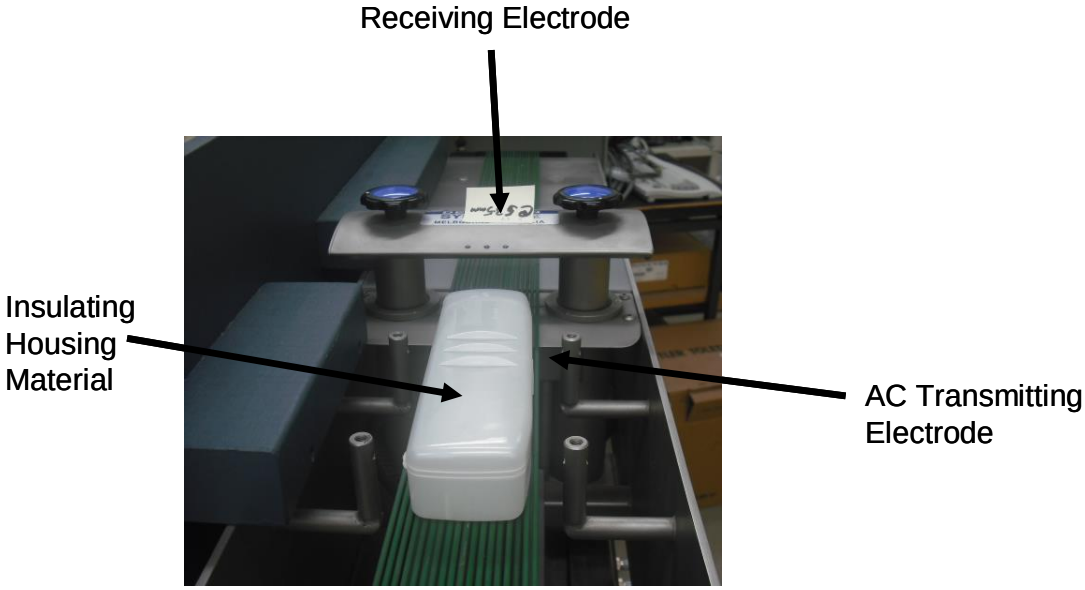

Figure 1: The WRF instrument used in this work. The sample to be analysed is placed in the insulating material (centre) and passed along the green carousel through the detection channel containing the transmitting and receiving electrodes.

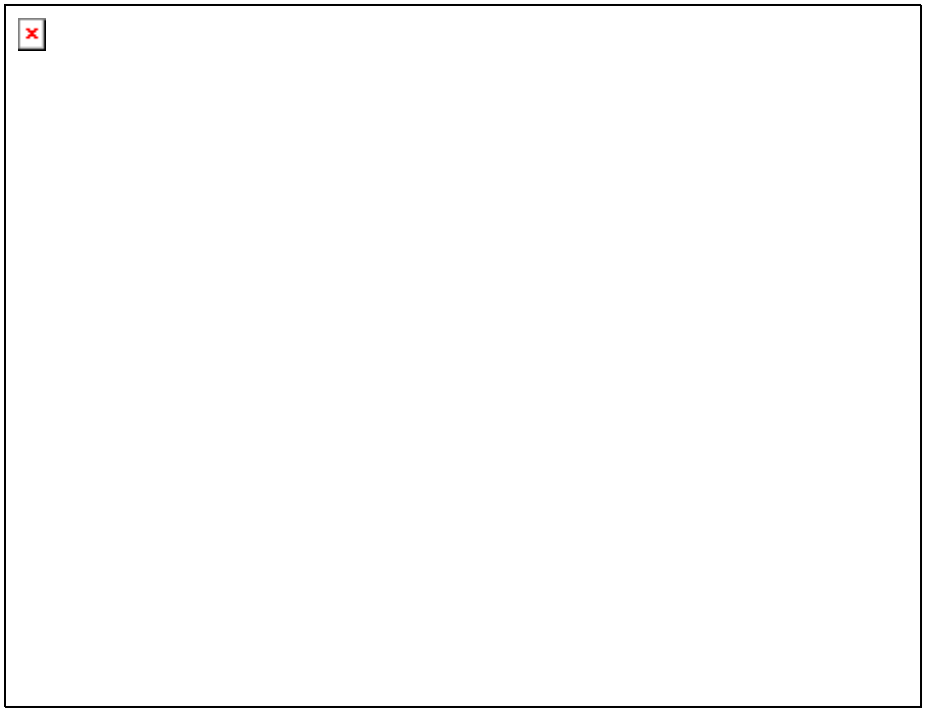

Figure 2: The individual responses obtained from WRF for membranes with component ratio 2:1, IL: PVC. Here the RF signal (y-axis) is given in arbitrary units.

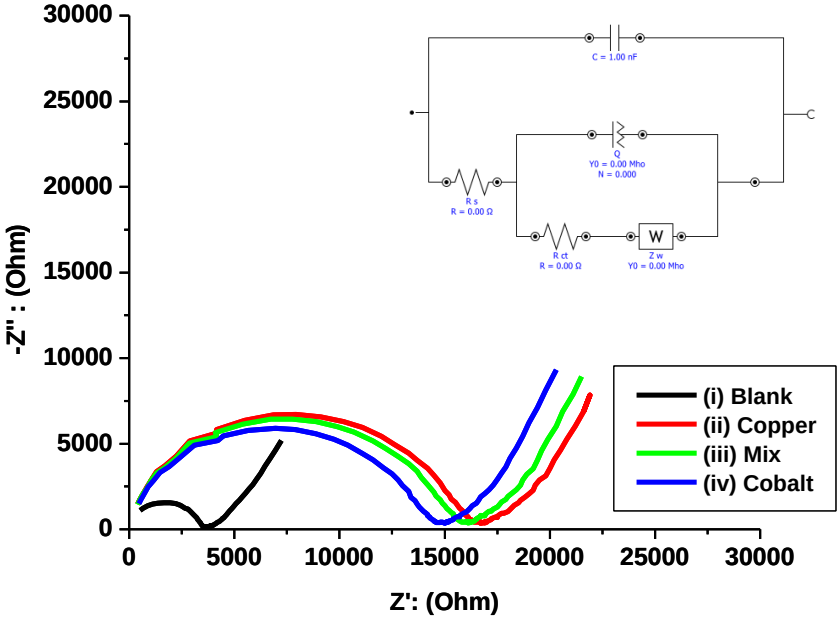

Figure 3: EIS spectra for membranes containing 2:1, IL:PVC; Here (i) is the blank (no metal ion exposure) run, whilst the coloured lines depict exposure to (ii) Cu^{2+} ions, (iii) a 1:1 (v/v) mixture of Cu^{2+} and Co^{2+} ions and (iv) Co^{2+} ions.

Inset: Equivalent "Randles" circuit representation used to obtain experimental data; where R_{CT} is the membrane resistance of charge transfer, Q is constant phase element and Z_W is Warburg impedance. "C 1nF" is the capacitance bridge used between the working and reference electrodes.

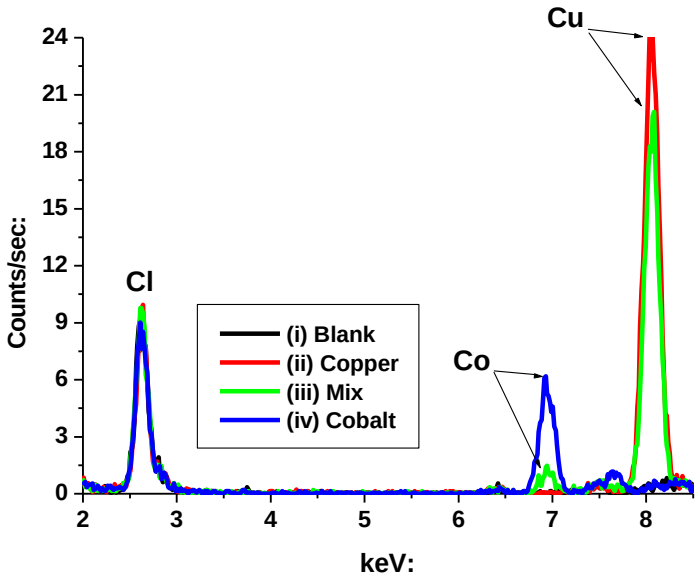

Figure 4: XRF spectra obtained for membranes with component ratio 2:1, IL: PVC. Here the black peaks are (i) no metal ion exposure (blank), whilst the coloured peaks correlate to membranes exposed to (ii) Cu^{2+} ions, (iii) a 1:1 (v/v) mixture of Cu^{2+} and Co^{2+} ions and (iv) Co^{2+} ions.

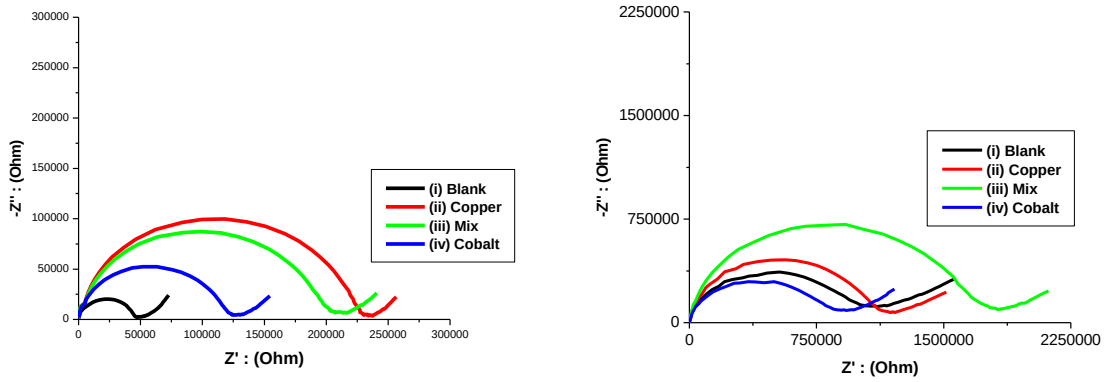

Figure 5: EIS results obtained for membranes containing 1:1, IL: PVC (left), and membranes containing 2:1, IL: PVC (right). For both cases; (i) no metal ion exposure (blank), (ii) exposure to Cu^{2+} ions, (iii) a 1:1 (v/v) mixture of Cu^{2+} and Co^{2+} ions and (iv) Co^{2+} ions.

Tables:

Membrane Composition:	***Blank:***	***Copper:***	***Mix:***	***Cobalt:***
2:1, IL: PVC	52486	39292	40267	43479

Table 1: Summary of WRF results for membranes containing 2:1 (IL : PVC); the values quoted are the result of peak area integration and mass correction analysis.

Membrane:	***R_{CT}: (Ω)***	***σ: (S/cm)***
Blank	3694	3.346×10^{-5}
Cobalt	15140	7.362×10^{-6}
Mix	16180	7.64×10^{-6}
Copper	16790	8.165×10^{-6}

Table 2: Resistance of charge transfer and conductivity values obtained via EIS analysis for membranes with component ratio 2:1, IL: PVC.

Membrane Composition:	***Blank:***	***Copper:***	***Mix:***		***Cobalt:***
	Cu *Co*		*Cu*	*Co*	
2:1, IL:PVC	192.55 <LOD	16996.25	12866.82	1559.59	7652.11
	(81.51)	(424.75)	(357.98)	(179.21)	(371.17)

Table 3: Concentration (ppm) values obtained from portable XRF analyser for membranes with component ratio 2:1, IL: PVC (errors in parentheses).

Membrane Composition:	***R_{CT}:(Ω)***	***σ : (S/cm)***
1:1, IL: PVC		
Blank	47760	7.649×10^{-6}
Copper	235600	1.551×10^{-6}
Mix	209900	1.74×10^{-6}
Cobalt	126400	2.89×10^{-6}
1:2, IL:PVC		
Blank	1,160,000	3.947×10^{-7}
Copper	1,200,000	3.816×10^{-7}
Mix	1,810,000	2.530×10^{-7}
Cobalt	919,000	4.982×10^{-7}

Table 4: Resistance of charge transfer and conductivity values obtained via EIS analysis for membranes with component ratio 1:1, IL: PVC (top) and 1:2, IL: PVC (bottom).

Membrane Composition:	***Blank:***	***Copper:***	***Mix:***	***Cobalt:***
1:1, IL: PVC	15879	7068	9428	14908
1:2, IL: PVC	7502	-	-	-

Table 5: Summary of WRF results for membranes membranes with 1:1, IL: PVC (top) and 1:2, IL: PVC (bottom). Again, the values quoted are the result of peak area integration and mass correction analysis.

Membrane Composition:	***Blank:***		***Copper:***	***Mix:***		***Cobalt:***
1:1, IL: PVC	*Cu*	*Co*		*Cu*	*Co*	
			2642.14	2551.91	272.17	1207.55
	>LOD	>LOD	(165.73)	(164.33)	(83.39)	(153.38)
1:2, IL: PVC	*Cu*	*Co*		*Cu*	*Co*	
			222.54	294.13	202.63	
	>LOD	>LOD	(77.79)	(90.91)	(88.09)	<LOD

Table 6: Concentration (ppm) values obtained from portable XRF analyser for membranes with component ratio 1:1, IL: PVC (top) and 2:1, IL: PVC (errors in parentheses).